ELSEVIER

# Temperature dependent polarized Raman spectra of nonaaqualanthanoid (Pr) single crystal

R.S. Jayasree [a,*], M.J. Bushiri [b], Annamma John [c], V.U. Nayar [d]

[a] Department of Imaging Sciences and Interventional Radiology, Sree Chitra Tirunal Institute for Medical Sciences and Technology, Trivandrum 695011, India
[b] Department of Physics, University of Kerala, Kariavattom, Trivandrum 695581, India
[c] Department of Physics, St. John's College, Anchal, Kollam 691306, India
[d] Department of Optoelectronics, University of Kerala, Kariavattom, Trivandrum 695581, India

## Abstract

Polarized Raman spectral changes with respect to temperature were investigated for $Pr(BrO_3)_3 \cdot 9H_2O$ single crystals. FTIR spectra of hydrated and deuterated analogues were also recorded and analysed. Temperature dependent Raman spectral variation have been explained with the help of the thermograms recorded for the crystal. Factor group analysis could propose the appearance of $BrO_3$ ions at sites corresponding to $C_{3v}$ (4) and $D_{3h}$ (2). Analysis of the vibrational bands at room temperature confirms a distorted $C_{3v}$ symmetry for the $BrO_3$ ion in the crystal. From the vibrations of water molecules, hydrogen bonds of varying strengths have also been identified in the crystal. The appearance $\upsilon_1$ mode of $BrO_3^-$ anion at lower wavenumber region is attributed to the attachment of hydrogen atoms to the $BrO_3^-$ anion. At high temperatures, structural rearrangement is taking place for both $H_2O$ molecule and $BrO_3$ ions leading to the loss of water molecules and structural reorientation of bromate ions causing phase transition of the crystal at the temperature of 447 K.
© 2005 Elsevier B.V. All rights reserved.

Keywords: Temperature dependent Raman spectra; Polarized Raman spectra; FTIR spectra; Hydrogen bonding; Phase transition

## 1. Introduction

The Nonaaqualanthanoid bromate crystallises in the hexagonal crystal system with space group $P6_3/mmc$ and has two formula units per unit cell [1]. The Pr ion co-ordinates with nine water oxygen atoms forming a tricapped trigonal prism (TCTP). Even though distorted TCTP's are rather common among the solid Ln compounds, the nona-aqua complex in the Ln bromate has the symmetry $D_{3h}$, one of the two idealised ground state geometries for nine co-ordination, the other being the $C_{4v}$ monocapped square antiprism.

Vibrational spectra of other hydrated rare earth bromates have been the subject of many investigators [2–4]. Vibrational spectra of rare earth (La, Nd and Gd) bromate nanohydrate crystals which form isostructural series with the title compound has been studied by Kato et al. and Poulet et al. [5,6].

In this paper, the polarized Raman spectra of $Pr(BrO_3)_3 \cdot 9H_2O$ at room temperature along with the FTIR spectra of hydrated and isotopically dilute analogues are presented. Temperature dependent Raman spectra of the crystal also have been recorded at four different temperatures and the spectral variation with respect to temperature have been discussed with supporting data of thermal analysis.

## 2. Experimental

Single crystals of $Pr(BrO_3)_3 \cdot 9H_2O$ (abbreviated as PrBH) were prepared by the procedure given by Albertsson and Elding by adding solid $KBrO_3$ to hot water solution of the respective perchlorates [1]. After cooling to about 15 °C, the precipitated $KClO_4$ was filtered off. Then slow

---

* Corresponding author. Tel.: +91 471 2443152x124/117 (O)/2478792 (R); fax: +91 471 2446433.
E-mail address: jayashreemenon@gmail.com (R.S. Jayasree).

evaporation at room temperature gave hexagonal crystals which were recrystallised several times in water. The isotopically diluted analogue was prepared by dissolving it in heavy water (99.% pure, BARC, Mumbai) and evaporating the solution in a vacuum desiccator. The process was repeated several times to enhance the percentage of deuteration.

A well grown single crystal was chosen and the crystallographic axes were determined using a polarizing microscope. The sides $x$, $y$ and $z$ of the crystal were chosen in accordance with crystallographic $a$, $b$ and $c$ axes. The sides of the crystal were cut, finely polished and properly aligned in the goniometer to record the Raman spectra in the 90° scattering geometry. The polarized Raman spectra were recorded in six crystal orientations, viz. $y(xx)z$, $x(yy)z$, $x(zz)y$, $y(xz)x$, $y(xy)z$ and $y(zy)x$. A 1401 Spex Raman spectrometer equipped with a Spectra Physics model 165.08 Ar$^+$ ion laser was used for recording Raman spectra using 514.5 nm exciting wave length at a resolution better than 3 cm$^{-1}$. Raman spectra of the crystal in $x(zz)y$ polarization were recorded at room temperature and at four different temperatures varying from 88 to 463 K. A variable temperature cell fitted with a thermocouple Pt-100 was used and the temperature of the crystal was determined at each stage. The FTIR spectra were recorded using a Burker IFS-66V FTIR spectrometer as polyethylene pellets (50–400 cm$^{-1}$) or KBr pellets (400–4000 cm$^{-1}$). The thermal analysis of the sample was carried out using a TA instrument (Model SDT 2960 simultaneous DTA–TGA) in the range 273–773 K.

## 3. Crystal structure and factor group analysis

The compound crystallises in the centrosymmetric space group $P6_3/mmc$. The structure is composed of columns of nona-aqua complexes linked by hydrogen bonds. Coordination polyhedron of $[Pr(H_2O)_9]^{3+}$ is a regular tricapped trigonal prism of symmetry $D_{3h}^1$. All the water molecules are hydrogen bonded to the O(3) atoms of bromate ion which are acceptors of three hydrogen bonds each. Of the six BrO$_3^-$

ions, four occupies site $C_{3v}$ while the other two occupies a site with higher symmetry, $D_{3h}$.

The factor group analysis [7] carried out predicts the existence of 237 modes at $k = 0$, excluding acoustic modes.

$$\Gamma_{PrBH} = 16A_{1g} + 12A_{2g} + 10B_{1g} + 18B_{2g} + 15E_{1g} + 17E_{2g} + 10A_{1u}$$
$$+ 17A_{2u} + 16 B_{1u} + 12B_{2u} + 16 E_{1u} + 15 E_{2u}$$

Details of the factor group analysis and correlation schemes for the internal modes of BrO$_3^-$ anions and water molecules are shown in Tables 1 and 2.

## 4. Results and discussion

FTIR and Raman spectra of PrBH are analysed and the assignments are done based on the vibrations of BrO$_3^-$ vibrations, water vibrations and lattice modes (Table 3). The polarized Raman spectra and FTIR spectra of the compound are given in Figs. 1–3. The temperature dependent Raman spectra are shown in Fig. 4.

### 4.1. BrO$_3^-$ vibrations

The normal modes of vibrations of a free BrO$_3^-$ ion with $C_{3v}$ symmetry are at 806, 421, 836 and 356 cm$^{-1}$ for the symmetric stretching $\upsilon_1(A_1)$, symmetric bending $\upsilon_2(A_1)$, asymmetric stretching $\upsilon_3(E)$ and asymmetric bending $\upsilon_4(E)$, respectively [8]. The vibrational representation of $XY_3$ planar $D_{3h}$ molecule is given as $\Gamma = A_1' + A_2'' + 2E'$ where only $\upsilon_2$, $\upsilon_3$ and $\upsilon_4$ are IR active and $\upsilon_1$, $\upsilon_3$ and $\upsilon_4$ are Raman active. In pyramidal systems with $C_{3v}$ symmetry, all the four frequencies $(2A_1 + 2E)$ are both infrared and Raman active [9].

The Br–O stretching region shows four bands in the Raman spectra of PrBH around 825, 805, 789 and 775 cm$^{-1}$. Bands at 825 and 789 cm$^{-1}$ exhibit high intensity while the bands at 805 and 775 cm$^{-1}$ appear as shoulders. Corresponding to these modes, in the IR spectrum, a highly intense band at 785 cm$^{-1}$ and a slightly less intense band

Table 1

Factor group modes of Pr(BrO$_3$)$_3$·9H$_2$O space group $P6_3/mmc(D_{6h}^4)$, $Z = 2$

|  | $A_{1g}$ | $A_{2g}$ | $B_{1g}$ | $B_{2g}$ | $E_{1g}$ | $E_{2g}$ | $A_{1u}$ | $A_{2u}$ | $B_{1u}$ | $B_{2u}$ | $E_{1u}$ | $E_{2u}$ |
|---|---|---|---|---|---|---|---|---|---|---|---|---|
| **Translational modes** | | | | | | | | | | | | |
| $[Pr(H_2O)_9]^{3+}$ | 0 | 0 | 0 | 1 | 0 | 1 | 0 | 1 | 0 | 0 | 1 | 0 |
| BrO$_3^-$ | 1 | 0 | 0 | 2 | 1 | 2 | 0 | 2 | 1 | 0 | 2 | 1 |
| **Vibrational modes** | | | | | | | | | | | | |
| $[Pr(H_2O)_9]^{3+}$ | 0 | 1 | 0 | 0 | 1 | 0 | 0 | 0 | 0 | 1 | 0 | 1 |
| BrO$_3^-$ | 0 | 2 | 1 | 0 | 2 | 1 | 1 | 0 | 0 | 2 | 1 | 2 |
| **Internal modes** | | | | | | | | | | | | |
| $[Pr(H_2O)_9]^{3+}$ | 12 | 9 | 9 | 12 | 8 | 10 | 9 | 12 | 12 | 9 | 10 | 8 |
| BrO$_3^-$ | 3 | 0 | 0 | 3 | 3 | 3 | 0 | 3 | 3 | 0 | 3 | 3 |
| **Acoustic modes** | 0 | 0 | 0 | 0 | 0 | 0 | 0 | −1 | 0 | 0 | −1 | 0 |
|  | 16 | 12 | 10 | 18 | 15 | 17 | 10 | 17 | 16 | 12 | 16 | 15 |

Table 2

Correlation scheme for the intramolecular vibrations of $Pr(H_2O)_9$ and $BrO_3$ in $Pr(BrO_3)_3 \cdot 9H_2O$

**(i)**    **$BrO_3$**      **n = 4**

| Free ion Symmetry $C_{3v}$ | Site Symmetry $C_{3v}$ | Factor Group Symmetry $\xrightarrow{\sigma_v}$ $D_{6h}$ | |
|---|---|---|---|
| 8   $A_1$ | $A_1$ | $A_{1g}$ | 2 |
| | | $B_{2g}$ | 2 |
| | | $E_{1g}$ | 2 |
| | | $E_{2g}$ | 2 |
| | | $A_{2u}$ | 2 |
| 16   $E$ | $E$ | $B_{1u}$ | 2 |
| | | $E_{1u}$ | 2 |
| | | $E_{2u}$ | 2 |

**(ii)**    **$BrO_3$**      **n =2**

| Free ion Symmetry | Site Symmetry | | Factor Group Symmetry | |
|---|---|---|---|---|
| $C_{3v}$ | $D_{3h}$ $\xrightarrow{}$ | $C_2'$ | $D_{6h}$ | |
| | $A_1'$ | | $A_{1g}$ | 1 |
| 4   $A_1$ | | | $B_{2g}$ | 1 |
| | | | $E_{1g}$ | 1 |
| | $E'$ | | $E_{2g}$ | 1 |
| | $A_2''$ | | $A_{2u}$ | 1 |
| | | | $B_{1u}$ | 1 |
| 8   $E$ | | | $E_{1u}$ | 1 |
| | $E''$ | | $E_{2u}$ | 1 |

**(iii)**    **$[P_r (H_2O)_9]^{3+}$**      **n = 2**

| Free ion Symmetry $D_{3h}$ | Site Symmetry $D_{3h}$ | Factor Group Symmetry $D_{6h}$ | |
|---|---|---|---|
| 24   $A_1'$ | $A_1'$ | $A_{1g}$ | 12 |
| | | $A_{2g}$ | 9 |
| 18   $A_2'$ | $A_2'$ | $B_{1g}$ | 9 |
| | | $B_{2g}$ | 12 |
| 40   $E'$ | $E'$ | $E_{1g}$ | 8 |
| | | $E_{2g}$ | 10 |
| 18   $A_1''$ | $A_1''$ | $A_{1u}$ | 9 |
| | | $A_{2u}$ | 12 |
| 24   $A_2''$ | $A_2''$ | $B_{1u}$ | 12 |
| | | $B_{2u}$ | 9 |
| 32   $E''$ | $E''$ | $E_{1u}$ | 10 |
| | | $E_{2u}$ | 8 |

Table 3
Polarized Raman and infrared frequencies of $Pr(BrO_3)_3 \cdot 9H_2O$

| x(zz)y | x(zy)y | x(xy)y | x(xz)y | y(xx)z | FTIR $H_2O$ | FTIR $D_2O$ | Assignments |
|---|---|---|---|---|---|---|---|
| 59m | 59w | | | 56vvw | 65w | 65w | |
| 80w | 78w | 79w | 75vw | 80vvw | 90w | 92w | Lattice modes |
| | 109w | 110w | 110w | | 110w | 110w | $\nu_6^c$ and $BrO_3^-$ libr |
| 120w | 129w | 128w | 128vw | 125vw | 126sh | 127w | |
| 156ms | 160mbr | 156mbr | 159mbr | 153mbr | 155w | 154w | $BrO_3^-$ rot. |
| | | | | | 168sh | 168 | |
| | 180sh | | | 180brmsh | | | $\nu_5^c$ |
| | | | | | 222m | 222w | $\nu_4^c$ |
| 378ms | 378ms | 380br | 380br | 372ms | 360vs | 361 | $\nu_4$ $BrO_3^-$ and $\nu_1^c$ |
| | 386sh | | | 385sh | 389m | 390 | |
| | | | 410vw | | | | |
| 432vw | 429vw | 430w | 432w | 429vw | 436s | 436 | $\nu_2$ $BrO_3^-$ and $\nu_3^c$ |
| 521vw | | | 546vvw | | | | lib. $H_2O$ |
| 773sh | 775shld | 771sh | 778sh | 775wsh | | | |
| 790vvs | 789s | 789vvs | 789s | 786ms | 785vs | 792 | $\nu_1 - \nu_3$ $BrO_3^-$ |
| 805sh | 800sh | 801sh | | 800sh | | | |
| 825vvs | 819vs | 825vs | 825vvs | 822s | 820sh | 819 | |
| | | | | | 1318w | | $\delta$ $D_2O$ and combinations |
| | | | | | | 1403 | |
| | | | | | | 1471w | |
| | | | | | 1595ms | 1596s | |
| 1610w | 1610 | | | | | | |
| | 1648vvw | | | | 1636m | | $\nu_2$ $H_2O$ |
| | 1659vvw | | | | | | |
| 1710vw | 1710vvw | | | | | | |
| | | | | | | 2531m | $\upsilon$ OD |
| | | | | | | 2573vw | |
| | | | | | | 2625m | |
| | | | | | 2850vw | 2849w | |
| 3055vvw | 3050vvw | 2970 | | | 2919vw | 2921w | |
| 3100w | 3080w | 3090w | 3078w | 3070m | | | |
| | | 3135vw | | | 3150sh | 3150 | |
| | 3230m | 3254vvw | 3230w | 3230w | | | $\nu_1 - \nu_3$ $H_2O$ |
| 3330w | 3348w | | | | | | |
| | 3418w | | 3410w | 3415w | | | |
| | | | 3450 | | 3456s | 3455 | |
| | | | 3499w | | 3518s | 3517 | |

$\upsilon^c - \upsilon$ $[Pr(H_2O)_9]^{3+}$; v, very; w, weak; s, strong; m, medium; sh, shoulder; br, broad.

at 820 cm$^{-1}$ are observed in this region [10]. On isotopical substitution, these bands appear as a broad band with two peaks at 792 and 819 cm$^{-1}$. In the Raman spectrum, the band at 789 cm$^{-1}$ appears to be highly polarized compared to the one at 820 cm$^{-1}$. Therefore, the 789 cm$^{-1}$ band is assigned to the $\upsilon_1$ mode and 825, ~805 and 775 cm$^{-1}$ bands are assigned to the $\upsilon_3$ modes.

In the bending mode region, nondegenerate $\upsilon_2$ mode is observed as a weak band at 430 cm$^{-1}$ in the Raman spectrum and as an intense band at 436 cm$^{-1}$ in the IR spectrum. The doubly degenerate $\upsilon_4$ mode appears with its degeneracy lifted in the $y(zy)x$ and $y(xx)z$ orientations of the Raman spectrum. In all other polarization orientations, this mode appears as a moderately intense singlet. In the IR spectrum also, two bands are observed at 360 and 389 cm$^{-1}$.

The appearance of all the four modes in both IR and Raman spectra suggests a $C_{3v}$ molecular symmetry for the $BrO_3^-$ ion in agreement with the conclusion of Hewett et al. [11].

The polarizability components $\alpha_{xx}$, $\alpha_{yy}$ and $\alpha_{zz}$ of $\upsilon_1$ ($BrO_3$) with $C_{3v}$ free ion symmetry belongs to the $A_{1g}$ and $E_{2g}$ species of the $D_{6h}$ factor group. Therefore, this mode is expected to appear in these species without distortion of the $BrO_3^-$ anion with $C_{3v}$ symmetry. However, this mode appears in all orientations with varying intensity. Distortion of the ion causes the appearance of this mode in all orientations of the crystal.

### 4.2. $H_2O$ vibrations

Stretching modes of water appear as weak bands in the 2970–3499 cm$^{-1}$ region of the Raman spectra. Three bands are observed in the $x(zz)y$ orientation whereas upto five bands are observed in other orientations. In the IR spectrum, three bands are observed at 3151, 3456 and 3518 cm$^{-1}$. Of these, the two bands at 3518 and 3456 cm$^{-1}$ appears as two equally intense bands whereas the other band appears as a weak one.
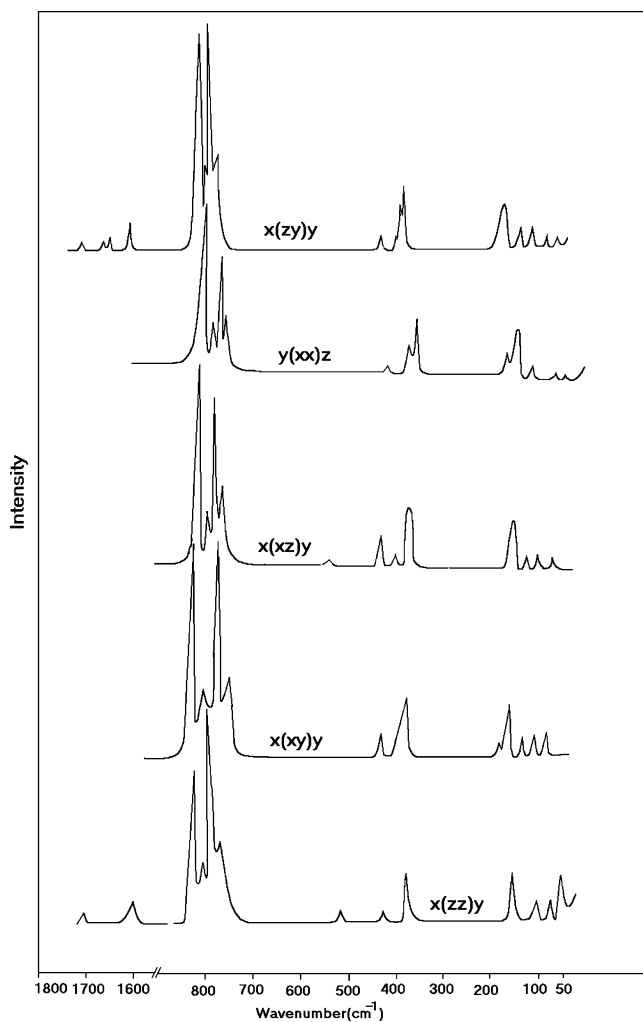
Fig. 1. Polarized Raman spectra of $Pr(BrO_3)_3 \cdot 9H_2O$ in various orientations [$x(zy)y$, $y(xx)z$, $x(xz)y$, $x(xy)y$ and $x(zz)y$] in the 50–1800 cm$^{-1}$ region.

On deuteration, no shift in frequency is observed for these bands. But additional three bands appear at 2626, 2573 and 2531 cm$^{-1}$ of which the one at 2531 cm$^{-1}$ may be due to HDO molecule.

In the bending mode region, four weak bands are observed in $y(zy)x$ polarization of Raman spectrum and two weak bands in the $x(zz)y$ polarization. This mode appears as a medium intense band at 1595 cm$^{-1}$ in the IR spectrum. On deuteration, this mode splits into two bands at 1595 and 1636 cm$^{-1}$. Additional three weak bands also appear at 1318, 1403 and 1471 cm$^{-1}$, again the band at 1471 cm$^{-1}$ corresponds to the vibrations of HDO molecule.

Appearance of multiple bands in the stretching mode region of water and the shifting of these bands to lower wavenumber side indicate the presence of hydrogen bonds in the crystal [12]. The large broadening observed to these bands in the IR spectrum is an indication of the presence of hydrogen bonds of varying strengths. Moreover, the presence of hydrogen bonding between the $BrO_3^-$ ion and water molecules
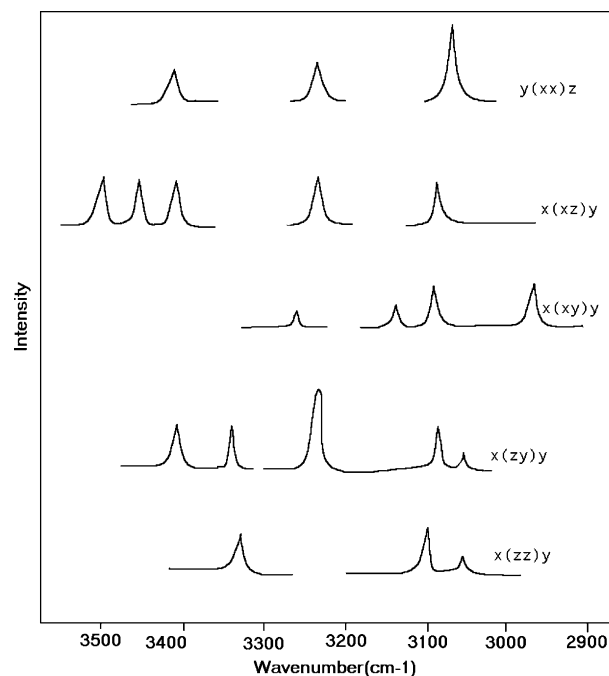


Fig. 2. Polarized Raman spectra of $Pr(BrO_3)_3 \cdot 9H_2O$ in various orientations [$y(xx)z$, $x(xz)y$, $x(xy)y$, $x(zy)y$ and $x(zz)y$] in the 2900–3600 cm$^{-1}$ region.

have been reported in compounds like Ln $(BrO_3)_9 \cdot H_2O$ where Ln = Nd, Gd and La [5,6]. In all these compounds, the lowering of symmetric stretching mode of $BrO_3^-$ group is observed due to the formation of hydrogen bonds similar to that in the present study. But, a shift in the $H_2O$ bending mode towards higher wavenumbers as observed in hydrogen bonded compounds is not observed here. This may
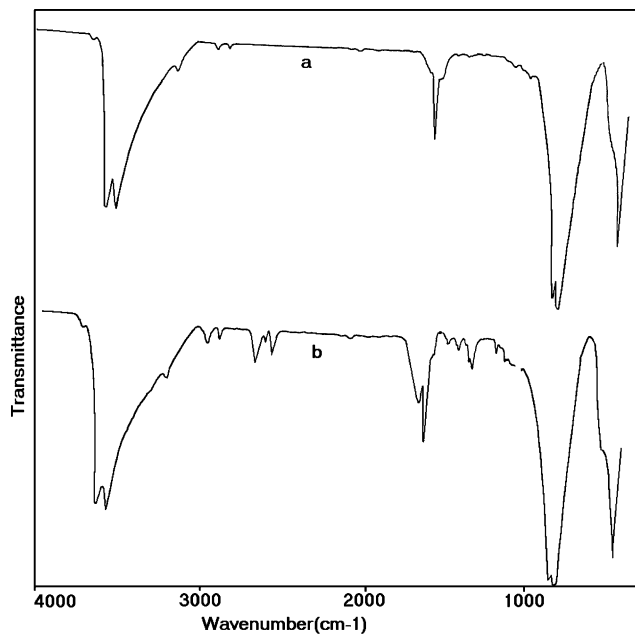


Fig. 3. FTIR spectra of $Pr(BrO_3)_3 \cdot 9H_2O$ (a) and $Pr(BrO_3)_3 \cdot 9D_2O$ (b).
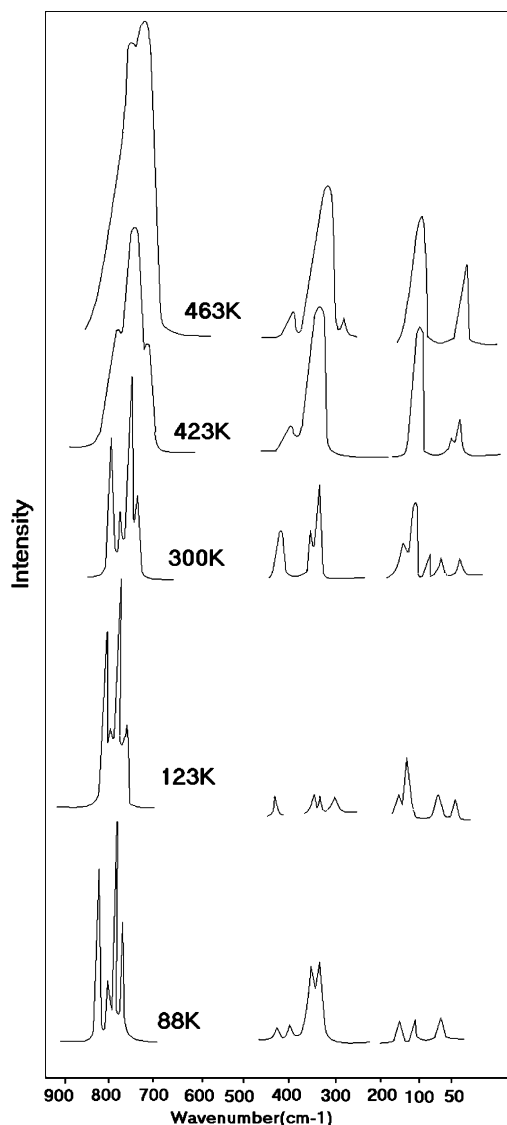
Fig. 4. Temperature dependent Raman spectra of $Pr(BrO_3)_3\cdot 9H_2O$ recorded in the $x(zz)y$ orientation in the 50–900 cm$^{-1}$ region.

Table 4
Raman frequencies of $Pr(BrO_3)_3\cdot 9H_2O$ at various temperatures

| Raman frequencies | | | | | Assignments |
|---|---|---|---|---|---|
| 300 K | 423 K | 463 K | 88 K | 123 K | |
| 76w | 74m | 74s | | 79vw | Lattice modes |
| | 89sh | | 84w | | |
| 106w | | | | | $\nu_6^c$ and $BrO_3^-$ libr. |
| 119w | | | 135w | 132w | |
| 160sbr | 159vsbr | 160vsvbr | 165w | 160m | $BrO_3^-$ rot. $\nu_5^c$ |
| 183wsh | | | | 180w | |
| | | 310vvw | | 310w | |
| 373s | | | 378ms | 375w | $\nu_4$ $BrO_3^-$ and $\nu_1^c$ |
| 389ms | 390vsvbr | 390svbr | 385mw | 389w | $\nu_2$ $BrO_3^-$ and $\nu_3^c$ |
| | | | 405vw | | |
| 435mbr | 442wbrsh | 450w | 435vw | 435vw | $\nu_1-\nu_3$ $BrO_3^-$ |
| 773ms | | | 775ms | 775m | |
| 793vvs | 789sh | | 789vs | 792vvs | |
| 805ms | 801vvsbr | | 805w | 807m | |
| 825vvs | 820sh | | 825vvs | 823vvs | |

$\nu^c-\nu$ $[Pr(H_2O)_9]^{3+}$; v, very; w, weak; s, strong; m, medium; sh, shoulder; br, broad.

ingly, a medium intense band is observed at 155 cm$^{-1}$ in the IR spectrum.

### 5.1. Temperature effects

Raman spectra of the crystal in the $x(zz)y$ polarization were recorded in 50–1000 cm$^{-1}$ region at 88, 123, 300, 423 and 463 K (Table 4). They are as shown in Fig. 4. DTA/TGA curves of the compound are shown in Fig. 5.



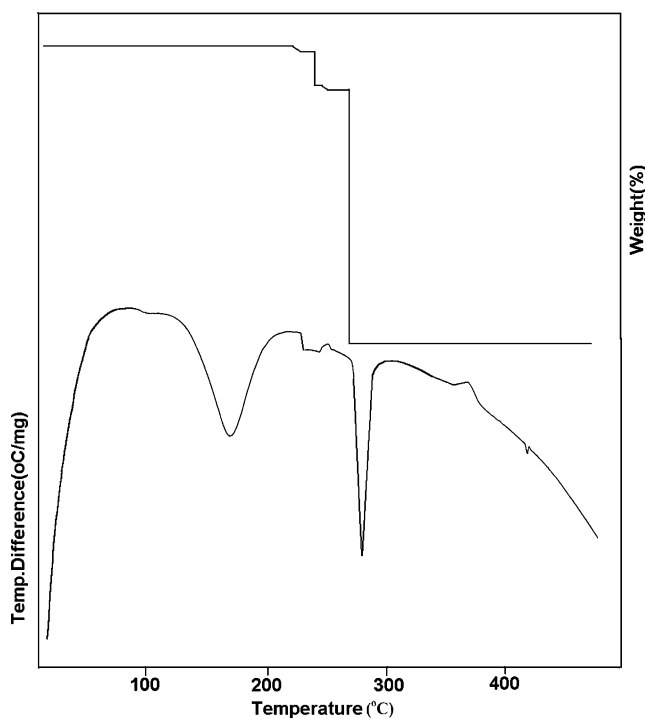Fig. 5. DTA and TGA curves of $Pr(BrO_3)_3\cdot 9H_2O$ from 33 to 500 °C (273–573 K).

be due to the metal oxygen co-ordination forming the tri-capped trigonal prism which tends to shift this mode towards the lower wavenumber values [12,13]. The appearance of the bending modes at frequencies as low as 1595 cm$^{-1}$ and as high as 1710 cm$^{-1}$ indicates the presence of distinct water molecules forming weak to very strong hydrogen bonds.

## 5. Lattice modes

Translational and rotational modes of $BrO_3^-$ ions and Pr atoms are observed below 300 cm$^{-1}$. An intense broad band appearing around 160 cm$^{-1}$ is assigned to the rotational modes since the rotational modes are more intense than the translatory modes in the Raman spectra [14]. Correspond-

## 5.2. High temperature phase

Raman spectra recorded at room temperature show four bands in the stretching mode region of $BrO_3^-$ ion at 773, 793, 805 and 825 $cm^{-1}$. When the temperature is raised to 423 K, the band at 773 $cm^{-1}$ disappears and the remaining three bands merge to form a very intense broad band appearing at 800 $cm^{-1}$ with two unresolved peaks on either side. The enhancement in intensity is calculated to be more than 300%. At 463 K, the band at 789 $cm^{-1}$ also disappears and a band appear with still enhanced intensity (>450%) with a peak at 819 $cm^{-1}$. The $\upsilon_2$ mode shift to 442 $cm^{-1}$ at 423 K and appears as a weak band. The intensity of this mode is again reduced at 463 K and the band shifts to 450 $cm^{-1}$. Even though Devanathan and Srinivasan [15] have reported that the $\upsilon_2$ mode of $BrO_3^-$ is unaffected by thermal treatment in $Cd(BrO_3)_2 \cdot 2H_2O$, a shift towards higher frequency region is observed in the present study. The doubly degenerate $\upsilon_4$ mode which appears as a doublet at room temperature is observed as a broad singlet extending from 350 to 410 $cm^{-1}$ with no increase in intensity. The weak band observed in the $H_2O$ bending mode region at 300 K disappears at 423 K. In the lattice mode region, the bands observed at 106, 119 and 183 $cm^{-1}$ are not observed in the high temperature spectra. At 463 K, a very weak band appears at 310 $cm^{-1}$ which is not observed at 300 or 423 K.

The thermogram shows a weight loss of 3.25% at 525 K. The weight loss is 15.72% at 554 K and near complete weight loss (99.96%) is observed at 557 K.

The DTA curve shows two intense exothermic peaks at 447 and 556 K and a medium exothermic peak at 511 K. The peaks at 556 and 511 K correspond to weight loss at the two temperatures. But, corresponding to the peak at 447 K, no weight loss is observed. This indicates that a phase transitional change occurs in the crystal at 447 K. The large enhancement in intensity of the Raman band at 800 $cm^{-1}$ along with considerable increase in band width and the disappearance of two bands in this region when compared to the room temperature spectra confirm a structural phase transition in the crystal. Removal of degeneracy of the $\upsilon_4$ mode further confirms this result, since $\upsilon_4$ mode is a sensitive probe which reflects changes in site symmetry as the crystal undergoes phase transition [16]. These structural changes can occur in the crystal due to the breaking up of hydrogen bonds. Water is becoming free and this causes the disappearance of $H_2O$ bending modes. Absence of the bands at 106, 119 and 183 $cm^{-1}$ in the lattice mode region of the high temperature spectra can be accounted for the disappearance of the lattice modes of water or a change in the selection rules due to an altered lattice structure at this temperature. Water molecules escape from the crystal starting from 525 K. As the hydrogen bonds are released, the $BrO_3^-$ groups in the crystal become either free anions or remain co-ordinated to the Pr atom. This may be the reason for the appearance of Br–O stretching frequencies towards higher frequencies at 463 K.

## 5.3. Low temperature phase

At 88 and 123 K, the width of Raman bands is reduced. They become sharp and distinct with slight enhancement in intensity. Out of the four bands observed in the $\upsilon_1$ and $\upsilon_3$ mode region, the intensity of the band at 789 $cm^{-1}$ is reduced slightly when compared to that observed at room temperature. The other three bands show no change in intensity. The intensity of the 373 $cm^{-1}$ band of the $\upsilon_4$ mode region ($BrO_3^-$) is reduced at 123 K to 80% of the intensity at room temperature. As the temperature is further reduced to 88 K, the intensity of this band is enhanced. The medium intense broad band at 435 $cm^{-1}$ corresponding to the $\upsilon_2$ mode becomes a weak band at 123 K. At 88 K, two weak bands appear at 425 and 405 $cm^{-1}$ for this mode. The narrowing of the bands and the changes in intensity at low temperature region can be attributed to the settling down of protons into more ordered positions in the crystal [17].

## 6. Conclusion

The appearance of all the four modes in both IR and Raman spectra suggests a $C_{3v}$ molecular symmetry for the $BrO_3^-$ ion. Distortion of the ion causes the appearance of $\upsilon_1$ mode in all polarization orientations. Appearance of a number of bands and the shifting of these bands to low wavenumber region with the large broadening of the stretching modes of water indicate the presence of hydrogen bonds of varying strengths in the crystal.

The large enhancement in intensity of the band at 800 $cm^{-1}$ along with considerable band width and the disappearance of two bands in this region compared to the room temperature spectra confirm a structural phase transition at 447 K. The narrowing of the bands and the changes in intensity at low temperature region is attributed to the settling down of protons into more ordered positions in the crystal.

## References

[1] J. Albertsson, I. Elding, Acta Cryst. B33 (1977) 1460–1469.
[2] T.K.K. Srinivasan, T. Devanthan, J. Raman Spectrosc. 21 (1990) 99–102.
[3] H.D. Lutz, H. Christian, W. Eckers, Spectrochim. Acta 41A (1985) 637–642.
[4] T.K.K. Srinivasan, T. Devanathan, J. Raman Spectrosc. 21 (1990) 91–98.
[5] Y. Kato, K. Okada, H. Fukuzak, T. Takename, J. Mol. Struct. 49 (1978) 57–70.
[6] H. Poulet, J.P. Mathiew, D. Vergnat, B. Vergnat, A. Hadni, X. Gerbaux, Phys. Status Solidi 32a (1975) 509–520.
[7] W.G. Fateley, F.R. Dollish, N.T. Mc Devitt, F.F. Bentley, Infrared and Raman Selection Rules for Molecular and Lattice Vibrations—The Correlation Method, Wiley, Interscience, New York, 1972.
[8] K. Nakamoto, Infrared Spectra of Inorganic and Co-ordination Compounds, second ed., Wiley, Interscience, New York, 1970.
[9] S. Mohan, K.G. Ravikumar, Indian J. Phys. 58B (1984) 8–14.
[10] M.J. Bushiri, V.U. Nayar, Spectrochim. Acta 58A (2002) 899–909.

[11] W.D. Hewett Jr., J.H. Newton, W. Weltner Jr., J. Phys. Chem. 79 (1975) 2640–2648.

[12] S.N. Vinogradov, R.H. Linnel, Hydrogen Bonding, Van Nostrand, Reinhold, New York, 1971.

[13] V.M. Malhotra, H.A. Buckmaster, H.D. Bist, Can. J. Phys. 59 (1980) 1667–1675.

[14] A. Viste, D.E. Irish, Can. J. Chem. 55 (1977) 3218–3227.

[15] T. Devanathan, T.K.K. Srinivasan, J. Solid State Chem. 73 (1988) 184–189.

[16] R.B. Wright, C.H. Wang, J. Phys. Chem. Solids 34 (1973) 787–795.

[17] R. Ratheesh, S. Suresh, M.J. Bushiri, V.U. Nayar, Spectrochim. Acta 51A (1995) 1509–1515.